Hydrol. Earth Syst. Sci. Discuss., 9, 11319–11361, 2012
www.hydrol-earth-syst-sci-discuss.net/9/11319/2012/
doi:10.5194/hessd-9-11319-2012

Hydrology and Earth System Sciences Discussions

Global multi-scale segmentation of continental and coastal waters from the watersheds to the continental margins

G. G. Laruelle[1], **H. H. Dürr**[2,4], **R. Lauerwald**[3], **J. Hartmann**[3], **C. P. Slomp**[2], **and P. A. G. Regnier**[1]

[1]Biogeochemical Modelling of the Earth System, Dépt. des Sciences de la Terre et de l'Environnement, Université Libre de Bruxelles, 1050 Bruxelles, Belgium
[2]Department of Earth Sciences – Geochemistry, Faculty of Geosciences, Utrecht University, The Netherlands
[3]Institute for Biogeochemistry and Marine Chemistry, KlimaCampus, Universität Hamburg, Bundesstrasse 55, 20146 Hamburg, Germany
[4]Ecohydrology Research Group, University of Waterloo, Canada

Received: 20 August 2012 – Accepted: 18 September 2012 – Published: 4 October 2012

Correspondence to: G. G. Laruelle (goulven.gildas.laruelle@ulb.ac.be)

Published by Copernicus Publications on behalf of the European Geosciences Union.

Abstract

The complex coastline of the Earth is over 400 000 km long and about 40 % of the world's population lives within 100 km of the sea. Past characterizations of the global coastline were constructed either from a continental perspective through an analysis of watershed river basin properties (COSCAT: Coastal Segmentation and related CATchments) or from an oceanic perspective, through a regionalization of the proximal and distal continental margins (LME: Large Marine Ecosystems). Here, we present a global-scale coastal segmentation, composed of three consistent levels, that includes the whole aquatic continuum with its riverine, estuarine and shelf sea components. Our work delineates comprehensive ensembles which retain the most important physical characteristics of both the land and shelf areas. The proposed multi-scale segmentation results in a distribution of global exorheic watersheds, estuaries and continental shelf seas among 45 major zones (MARCATS: MARgins and CATchments Segmentation) and 149 sub-units (COSCATS). Geographic and hydrologic parameters such as the surface area, volume and fresh water residence time are calculated for each coastal unit as well as different hypsometric profiles. Our analysis provides detailed insights into the distributions of coastal and continental shelf areas and how they connect with incoming riverine fluxes. These results can be used for regional analyses and combined with various typologies for upscaling and biogeochemical budgets. In addition, the three levels segmentation can be used for application in Earth System analysis.

1 Introduction

The coastal zone is one of the most complex constituents of the biosphere and is a particularly active interface due to contrasting terrestrial and marine influences (Gattuso et al., 1998; Mackenzie et al., 1998). Inputs of terrestrial material such as sediment loads and nutrient fluxes through rivers and groundwater discharge are – to a varying degree – filtered and recycled in coastal areas. Coastal currents and major oceanic features, e.g. in upwelling areas, further re-shape this exchange and lead to major transformations of energy and matter before, ultimately, the open ocean is reached (Alongi 1998; Jahnke, 1996; Mackenzie et al., 2002, 2005; Slomp and Van Cappellen, 2004; Wollast, 1998). Depending on the interplay between the geomorphological settings, shapes and hypsometric profiles, together with climatic and hydrodynamic influences, key processes and transformations of many global biogeochemical cycles are played out in coastal waters (Arndt et al., 2011; Cai et al., 2011; Laruelle et al., 2009; Liu, 2010; Mackenzie, 1981; Smith and Hollibaugh, 1993; Wollast, 1983). 18 % of the marine primary production takes place in the continental shelf seas (Biscaye et al., 1994) and is sustained by both the nutrient delivery from continents via the rivers (Seitzinger et al., 2005) as well as coastal upwelling (Longhurst et al., 1998). The relative shallowness of coastal waters, compared to the open ocean is also responsible for intense coupling between pelagic and benthic processes (Crossland et al., 2005; Mackenzie et al., 1998). They also are the siege of important carbon and nutrient burial within aquatic sediments (DeMaster et al., 2002; Rabouille et al., 2001; Seiter et al., 2005).

Yet, definitions of the coastal zone and its geographical extent often vary from one study to another, largely depending on the background of the observer and the purpose of the research. Oceanographers and marine scientists often neglect near-shore features such as estuaries and regularly use the term of coastal zone when referring to the continental shelf as a whole (Crossland et al., 2005; Smith and Hollibaugh, 1993). In terms of material fluxes at the land-ocean interface and from a marine perspective, the continental shelves act as a filter between inland waters and the open ocean. They are, in fact, a succession of nested filters for water and associated material transported by rivers or groundwater, the first one being estuaries (Elliott and Mc Lusky, 2002; Woodwell et al., 1973) and the last one being large regional seas (Meybeck et al., 2007). However, the location of the limit between rivers and estuaries is not always easy to determine and the entire aquatic cycle can be considered a continuous system. In fact, rivers, estuaries and continental shelves seas can be viewed as a succession of tightly connected systems where individual boundaries are blurred by the strong spatial gradients and high temporal variability in temperature, salinity, and chemical elements concentrations.

Nevertheless, segmentation is a critical step when making budgets of water and bio-active elements for coastal systems (Dürr et al., 2011; Laruelle, 2009; Laruelle et al., 2010; Meybeck et al., 2006). For instance, global segmentations of coastal regions have been developed for purposes as diverse as benthic carbon budgeting (Seiter at al., 2005) or fish resource management (Large Marine Ecosystems, LME; Sherman et al., 1989; Sherman, 1991). In the LME segmentation, the outer boundaries can stretch well beyond the geographical limit of the continental shelf and the boundaries used to delineate their regional oceanic provinces are determined using a fisheries management or other political perspective rather than using a set of consistent natural criteria such as geomorphological features or currents. Another approach came with the LOICZ program which compiled information from the contributing terrestrial area to the coast and beyond the continental margins. The LOICZ approach does not, however, propose a spatially-explicit segmentation in geographical units. For instance, the COSCAT approach (Coastal Segmentation and related CATchments) created by Meybeck et al. (2006) distinguishes different segments of the global coastline based on a combination of terrestrial watershed characteristics. In the recent synthesis by Liu (2010), the coastal ocean has been segmented using large scale coastal currents and climatic zones and Dürr et al. (2011) proposed a distinction of estuaries along criteria relating their shape to the filtering function for riverine material.

However, at global scale, a spatially-explicit segmentation that incorporates consistently the main features of both the land and the ocean realms remains to be performed. A major difficulty in this context consists in accounting for the difference in spatial scales between the linked aquatic and costal systems. For instance, estuaries are a fundamental component of the land-ocean continuum because of their filtering capacity with respect to carbon, nutrients and sediment (Arndt et al., 2007, 2009; Laruelle, 2009; Laruelle et al., 2009; Nixon et al., 1996; Regnier, 1999; Vanderbrought, 2002, 2007).

HESSD
9, 11319–11361, 2012

Yet, with typical length and width scales of 10 to 100 km and 1 to 10 km, respectively, they are much smaller entities than large scale coastal oceanic currents such as the Gulf Stream or the California current which flow along continents over thousands of kilometers (Longhurst, 1998). Thus, a multi-scale approach is required to capture the complexity of the Land-Ocean continuum.

In this study, we present a harmonized multi-scale segmentation for global continental waters which updates and combines existing approaches, including the complete suite of connected systems from the watershed to the outer limit of the continental shelf. It is based on three levels of increasing spatial resolution. The first level (0.5° resolution) involves the main riverine watersheds and identifies the dominant type of estuarine filter. Following the typology of Dürr et al. (2011), estuarine types follow a nomenclature distinguishing between small deltas, tidal systems, lagoons and fjords. The second level is based on an updated version of the COSCAT segmentation (Meybeck et al., 2006). This is then extended to include the adjacent continental shelves. The highest level in the hierarchy is termed MARCATS (for MARgins and CATchment Segmentation) and consists of aggregated COSCAT units according to the main climatological, morphological and oceanographic characteristics of the coastal zone. The two highest levels of our segmentation are used to calculate surface areas and volumes for the entire coastal ocean along hypsometric profiles for different isobaths. Within each segment, fresh water flow (i.e. river discharge) is used to calculate fresh water residence times as well as the partitioning of fresh water discharges between the different types of estuarine ecosystems.

2 Segmentation: limits and definitions

The present study describes a segmentation of continental waters based on three levels of increasing aggregation. The finest segmentation corresponding to the lowest level of aggregation (level I) resolves the 0.5° river network of Vörösmarty et al. (2000a, b). It includes all inland waters and is used here as a canvas for a coarser aggregation

HESSD
9, 11319–11361, 2012

which consists in a grouping of riverine watersheds on the continental side and the delineation of contiguous continental shelf segments on the oceanic side (Fig. 1). This intermediate level of aggregation is based on an updated version of the COSCAT segmentation developed by Meybeck et al. (2006), (level II). Finally, the merging of COSCATs units into larger entities called MARCATS provides the coarsest segmentation (level III).

2.1 COSCAT segmentation and GIS calculations

The COSCATs are homogeneous geographical units which are independent of administrative borders. They primarily rely on lithological, morphological, climatic and hydrological parameters to partition the global coastline into segments with similar properties. The total number of COSCAT units amount to 149 for an average coastline length of 3000 km. Meta-watersheds attributed to each coastal segment are constituted of all the individual watersheds whose rivers discharge within the corresponding COSCAT. Following Laruelle et al. (2010), each COSCAT is also associated with a section of the continental shelf adjacent to the coastline. The lateral boundaries of a specific shelf unit are defined by perpendicularly extrapolating the limits of the corresponding coastal segment from the shoreline to the 1000 m isobaths, extracted from 1' resolution global bathymetries (see below). Where the limit between two COSCATs on the shelf corresponds to a major topographic feature such as a submarine ridge or the connection between two oceanic basins, this feature is used as boundary instead. For the purpose of the study, a number of minor modifications were applied to the original COSCAT boundaries, to account for stretches of coasts with similar estuarine characteristics (Dürr et al., 2011) or the profile of some continental shelves. The COSCAT 401 running from the Gibraltar strait to the Atlantic border between France and Spain was split into two segments (COSCATs 401 and 419) corresponding to the Northern and Western Iberic coasts, respectively. The COSCATs 414 and 1302, corresponding to the European and Asiatic coasts of the Aegean Sea were merged. The boundary between COSCATs 1111 and 1112, at the Southern edge of South America in the Pacific was

HESSD
9, 11319–11361, 2012
Global multi-scale segmentation of continental and coastal waters
G. G. Laruelle et al.

moved northward to account for the change in estuarine types from fjords to arheic (Dürr et al., 2011). In addition, all endorheic watersheds were excluded from the study. This concerns the four COSCATs segments flowing into the Aral and Caspian Seas (410, 1304–1306). The Antarctic continent, on the other hand, was included here using five new COSCATs (1501 to 1505). A map of all the COSCAT segments and their updated limits is provided as supplementary material.

The isobaths on continental shelves were extracted from 1' resolution global bathymetries. The version 9.1 of the bathymetry of Smith and Sandwell (1997, updated in 2007, http://topex.ucsd.edu/marine_topo) was preferably used as it generally better represents very near shore coastal features (Dürr et al., 2011). However, its geographical coverage does not extend past 80° North and South. Beyond this limit, the isolines were then extracted from the ETOPO 2 bathymetry (US Department of Commerce, National Oceanic and Atmospheric Administration, National Geophysical Data Center 2006, http://www.ngdc.noaa.gov/mgg/fliers/06mgg01.html). In the Northern Hemisphere, this concerns the Northern part of the Canadian archipelagos and Greenland as well as the Russian Arctic shelves. In the Southern Hemisphere, it only affects Antarctica. Ten isobaths were extracted for each COSCAT: 20 m, 50 m, 80 m, 120 m, 150 m, 200 m, 350 m, 500 m, 750 m and 1000 m. After a conversion from grid data to vector polygons using GIS, the surface area and average water depth was calculated for each polygon. The aggregation of polygons for each COSCAT provides the surface area and the volume of a shelf segment comprised between two isobaths. Table 1 provides the globally integrated surface areas and volumes of the continental shelves for the succession of depth intervals.

For each COSCAT, the depth at which the shelf breaks was estimated by calculating the slope of the sea floor. The outer limit of the shelf was defined as the isobath for which the increase in slope is the maximum over the 0–1000 m interval, yet still inferior to 2 %. This value was selected as a compromise between the average slope and the upper continental slope of 0.5 and 3 %, respectively, although the latter varies between 1 % and 10 % (Gross, 1972; Pinet, 1996). Locally, some very irregular topographic

HESSD
9, 11319–11361, 2012

features smaller than the spatial resolution of our bathymetric grid induced artifacts which required manual corrections based on geographic atlases (New York Times, 1992).

2.2 MARCATS segmentation

The coarsest segmentation (level III) aggregates COSCAT units into larger geographical boundaries whose limit account for oceanic features such as coastal currents or the pursue of marginal seas. The resulting 45 units (Fig. 2), named here MARCATS, are an aggregation of 3–4 COSCATs on average. Some MARCATS, however, correspond to one COSCAT only when they represent a well defined coastal feature like the Leeuwin current (MARCATS 33, LEE) which flows Southward off the coast of Australia and differs in nature from adjacent COSCATs (Pearce, 1997). On the other hand, some MARCATS are an aggregation of up to 10 COSCATs in the case of a large marginal sea like the Mediterranean Sea (MARCATS 20, MED). Each MARCATS was attributed a type following Liu's classification of continental shelf seas (Liu et al., 2010). The different classes are: Eastern Boundary Current (EBC, 1), Western Boundary Current (WBC, 2), Sub-polar Margins (3), Polar Margins (4), Monsoon influenced Margins (5), Marginal Seas (6), Tropical Margins (7).

Eastern and Western Boundary currents (1 and 2) are generated by large oceanic gyres when they flow parallel to the continents. The lateral water flow created by Ekman's current perpendicular to the boundary current induces upwelling of deeper waters which sustain primary production where the upwelling flux is large enough (Atkinson et al., 2005). Monsoon dominated margins (3) regroup all Indian Ocean's coasts where the hydrodynamics are strongly driven by the seasonal wind patterns of the Monsoon (Nag, 2010). Sub-polar margins (4) are characterized by cool temperate waters located on latitudes higher than 50° North and lower than 30° South approximately. These limits are used to differentiate them from the Polar margins (5) which explicitly refer to coastal waters surrounding the Arctic and Antarctic oceans. Marginal seas (6) refer to interior seas constituted of shallow waters belonging to the continental shelf

HESSD
9, 11319–11361, 2012

(Hudson Bay, Baltic Sea, Persian Gulf) or wider entities including deep waters (Gulf of Mexico, Mediterranean Sea, Sea of Japan...). In this case, the MARCATS only represent the generally narrow shelves surrounding the main regional sea. An important characteristic of such marginal systems is a generally longer renewal rate of water compared to other systems directly connected to the open ocean (Meybeck and Dürr, 2009). Last, tropical margins (7) are typically warm coastal waters located in the tropics and forming an equatorial belt around the Earth. The average temperature in such areas is high (> 18 °C) all year long regardless of seasonality. Note that some coastal regions present characteristics corresponding to several classes. For instance, the Red Sea could arguably be defined as a marginal sea influenced by the Monsoon. In such cases, a hierarchy of criteria was used to identify the dominant characteristic. The first criterion is the occurrence or absence of EBC or WBC. Next, the presence of a Marginal Sea is used and, finally, monsoonal influence is applied. There is no overlap between the three remaining classes (Tropical, Polar and Sub-Polar).

3 Results and discussion

3.1 MARCATS classification of continental shelves

Figure 2 presents the location and surface area of the 45 MARCATS units. Table 2 lists all the MARCATS and their constitutive COSCATs for which the shelf break depth is also given. The limits of the individual COSCATs are also represented by black lines in Fig. 2. The color code corresponds to the MARCATS classification, the continental shelves being highlighted in slightly darker colors. Note that the geographic projection used for this map over-represents the surface area of high latitude regions – this has been corrected for in the surface area and volume calculations. EBC and WBC (in orange and yellow, respectively) border most continents at the mid latitudes and account for a cumulative coastline of over 70 000 km. The major upwelling regions (California, Morocco, Canary, Humboldt and so forth...) are driven by EBC or WBC; yet these

HESSD
9, 11319–11361, 2012

currents generally follow the continents over much larger distances than those corresponding to the area where upwelling is intense (Longhurst, 1995, Xie and Hsieh, 1975). In the Pacific, the MARCATS 2 (CAL) and 4 (HUM) exemplify this feature. They comprise five and three COSCATs, respectively, while in reality, only one COSCAT covers the high intensity upwelling area (COSCAT 805 for the Californian Current and COSCAT 1114 for the Humboldt Current, Table 2). The Californian current, for instance, is a part of the North Pacific Gyre which extends up to the latitude corresponding to British Columbia in Canada (Karl, 1999; Mann and Lazier, 2006) although the upwelling is induced along the South Western coast of the United States. In the Atlantic, Northern Hemisphere EBCs are located is the zone along Senegal to the Iberian Peninsula, and producing the Morocco (MARCATS 22, MOR) and Portugal upwellings (MARCATS 19, IBE). In the Southern Hemisphere, the EBC is located off the coast of Namibia (Benguela Current, MARCATS 24, SWA). The only EBC in the Indian Ocean is the Leeuwin current, located along the Western border of Australia (MARCATS 33, LEE). The distribution of WBCs essentially mirrors that of EBCs on the opposite side of the oceans. In the Pacific ocean, South East Asia is bordered by a WBC in the North (MARCATS 39, CSK) and the South (MARCATS 35, EAC), respectively. In the Atlantic, the Brazilian (MARCATS 6, BRA) and the Florida currents (MARCATS 10, FLO) are the pair of WBCs, one per hemisphere. Finally, in the Indian Ocean, the Southern tip of Africa is associated with the Agulhas current which flows from Madagascar to Cape Town (MARCATS 25, AGU).

Margins under monsoonal influence (green) account for about half of the length of the shelves in the Indian Ocean, forming a 20 000 km long arc running from the coast of Somalia (MARCATS 27, WAS) to the Bay of Bengal (MARCATS 31, BEN) which also includes all the coast of India (MARCATS 30, EAS). The main characteristic of this region is the seasonal inversion of wind patterns, affecting the climate as well as the direction and strength of coastal currents. As a consequence, the coast of Somalia is an area of upwelling in the summer (Longhurst, 1998) as this region is influenced by a seasonal boundary current which disappears during winter time.

HESSD
9, 11319–11361, 2012

Subpolar margins (light blue) are found on all continents but Africa. They are located at relatively high latitudes (above 40–50°) in regions where EBCs and WBCs fade out or drift away from the coasts. In the North Pacific, the subpolar margins lie along the Western coast of Canada and South Alaska (MARCATS 1, NEP) and on the Eastern face of Russia (MARCATS 42, NWP). The Southern portion of South America is also considered sub-polar and extends from the northernmost fjords of Chile on the Pacific side to the Rio de la Plata on the Atlantic side (MARCATS 5, SAM). A large fraction of the North Atlantic is bordered by sub-polar shelves including the Labrador Sea (MARCATS 11, LAB), Southern Greenland (MARCATS 15, SGR) and North Western Europe (MARCATS 17, NEA). The latter comprises Southern Iceland, as well as the Irish, Celtic and North Seas. On the antipodes, Southern Australia (MARCATS 34, SAU) and New Zealand (MARCATS 36, NWZ) complete the world distribution of subpolar margins.

Polar margins (deep blue) are located at very high latitudes of the Northern Hemisphere and include the Canadian archipelagos (MARCATS 13, CAN), Northern Greenland (MARCATS 14, NGR), the Norwegian basin (MARCATS 16, NOR) and the Russian Arctic Ocean (MARCATS 43, SIB and 44, BKS). In the Southern Hemisphere, the Antarctic continent is bordered by the polar MARCATS 45 (ANT).

In our classification, Marginal seas (purple) include all enclosed and semi-enclosed shelves. All of them are located in the Northern Hemisphere and they can be subdivided into two broad categories. The first category consists of the shelves bordering large deep oceanic basins such as the Gulf of Mexico (MARCATS 9, MEX), the Sea of Japan (MARCATS 40, JAP) and the Okhotsk Sea (MARCATS 41, OKH). The Black Sea (MARCATS 21, BLA), the Mediterranean Sea (MARCATS 20, MED) and the Red Sea (MARCATS 28, RED) also consist of narrow shelves surrounding deeper waters but, in addition, they are characterized by a very limited connection to the ocean. In spite of being defined as a marginal sea, the influence of monsoon wind patterns can be observed in the hydrodynamics of the Southern Red Sea (Al-Barakati et al., 2002). The other category of Marginal Seas consists of inner continental bodies of relatively

HESSD
9, 11319–11361, 2012

shallow waters such as the Hudson Bay (MARCATS 12, HUD), the Baltic Sea (MARCATS 18, BAL) and the Persian Gulf (MARCATS 29, PER).

The remaining margins are located between both tropics (red). They are aligned in a sort of Equatorial belt around the Earth and include the Pacific and Atlantic coasts of Central America (MARCATS 3, TEP and MARCATS 7, TWA), the Caribbean Sea (MARCATS 8, CAR), the Atlantic and Indian coasts of Central Africa (MARCATS 23, TEA, and 26, TWI) as well as a large section of Oceania running from the North of Australia to the South of China and comprising most of Indonesia and the Philippines (MARCATS 37, NAU).

3.2 Global importance of the continental margins

Table 1 provides global values for sea surface areas and water volumes between the different isobaths used in this study. The global surface area of 26×10^6 km^2 between the coastline and the 200 m isobath (the commonly used outer limit for the coastal ocean in global studies, Walsh, 1988; Borges et al., 2005) is similar to that of Laruelle et al. (2010). Yet, the distribution of this area among depth intervals indicates that the portion shallower than 80 m contributes to 17×10^6 km^2. A significant fraction of the continental margins thus corresponds to shallow coastal waters such as the wide North Sea (COSCAT 404), the Patagonian and Arctic continental shelves. The latter two exhibit highly extended shallow surface areas (< 200 m) followed by a gentle slope and a deep shelf break.

Most coastal ocean surface area evaluations yield values in the range $25–30 \times 10^6$ km^2 (Laruelle et al., 2010; Walsh et al., 1988; Cai et al., 2006; Chen and Borges, 2005), which corresponds to 8 % of the world's ocean (Rabouille et al., 2005). Nonetheless, the common definition of a single proper limit for the outer edge of the continental shelf is still a matter of debate in the literature (Borges et al., 2005; Laruelle et al., 2010; Liu, 2010). The choice of this limit depends on various sedimentological and morphological criteria but also, to some degree, on convenience of use. Convenience is the main reason why the 200 m isobath has often been selected as it provides a

HESSD
9, 11319–11361, 2012

consistent limit which is easy to manipulate and allows for inter-comparability between studies. Liu et al. (2010) proposed a definition based on the increase in slope of the continental shelf as an alternative. This definition is also used here (see Sect. 2.1) and although our estimate of 30×10^6 km^2 falls within the range of previously reported values, the method allows for a more rigorous regional analysis of the shelf area distribution around the globe. The shelf break depths for each COSCAT are provided in Table 2. Furthermore, the surface areas and volumes between the calculated isobaths for all COSCAT segments are available as supplementary material. In particular, this allows for comparisons between studies relying on different definitions for the boundary of the coastal ocean.

The integrated volume of all continental shelves, from the shore to the shelf break, is 3860×10^3 km^3 (for a surface area of 30×10^6 km^2). Most continental shelves break at water depths between 150 m and 350 m (Fig. 3). The deeper shelves are found in polar and sub-polar regions and their integrated volume accounts for more than half of the world's total volume of the coastal ocean. This includes the shelves of Antarctica which are very deep and extend down to 1000 m. Such particularity is a result of the downwarping caused by the weight of the ice sheet on the continent, glacial erosion and the lack of sedimentation from fluvial discharge (Anderson, 1999). It also includes the very wide Arctic shelves. Tropical shelves are generally shallower whereas shelves in contact with EBCs and WBCs do not exhibit a clear trend. Regions under monsoonal influence all have a shelf limit between 150 m and 350 m. Internal marginal seas such as Hudson Bay, the Baltic Sea and the Persian Gulf (HUD, BAL and PER) are relatively shallow and are entirely comprised within the continental platform. Therefore, they do not break and are not included in the accounting of COSCATs in Fig. 3a. In Fig. 3b, HUD, BAL and PER were assigned to the range corresponding to their maximum water depth, excluding any highly localized deep features (< 5 % of surface area). The bulk of this distribution consists of relatively deep shelves. This is explained, in part, by the significant contribution of the deep Arctic shelves which amount to 5×10^6 km^2 alone. It also indicates that many shallow shelves are relatively narrow. This is particularly

HESSD
9, 11319–11361, 2012

Global multi-scale segmentation of continental and coastal waters

G. G. Laruelle et al.

striking for EBC which only represent a total surface area of 1.2×10^6 km^2 and, to a lesser extent, WBC with a total surface area of 2.9×10^6 km^2.

3.3 Connecting MARCATS with the continents

Table 3 summarizes the surface areas of watersheds, estuaries and continental shelves for every MARCATS. The surface areas of estuarine systems are based on a spatially explicit typology consisting of four different types of active estuarine filters and three types where estuarine filtering is absent (Dürr et al., 2011). Type I consists of small deltas and miscellaneous secondary streams or transitional systems which exhibit very limited filtering capacities. Type II regroups all estuaries and embayments dominated by tidal forcing. This includes all macro-tidal estuaries and bays but also most rias and many meso-tidal systems like those found in Southern Atlantic America and Siberia. Type III represents lagoons and enclosed estuaries, relatively protected from tidal influence (Schwartz, 2005). Type IV comprises fjords, fjaerds and other miscellaneous high latitudes systems generally characterized by deep waters and very long fresh water residence time. Large rivers (Type V) often produce an estuarine plume that protrudes past the conventional geographical limits of estuaries and, sometimes, even of continental shelves (McKee et al., 2004). To attribute a surface area to each estuarine type within each MARCATS, the respective length of each estuarine class is multiplied by an average ratio of estuarine surface per km of coastline following the procedure of Dürr et al. (2011). The distribution of estuarine types varies widely amongst the different classes of MARCATS. The Polar margins in the Northern Hemisphere contribute 31 % to the estuarine surface areas (10^6 km^2). These estuaries are heavily dominated by fjords (Fig. 4a). Antarctica does not have any estuary according to this calculation because the few rivers are essentially meltwater streams (Anderson, 1999; Jacobs et al., 1992).

The world's exorheic watershed surface totals 113×10^6 km^2, which is 4 times larger than that of continental shelves and more than 100 times that of estuaries (Fig. 4b).

HESSD
9, 11319–11361, 2012

Naturally, the ratio between these surfaces significantly varies from one region to another as well as the estuarine distribution along the coast. The spatial distribution of estuarine systems is indicated in Fig. 5a–f. Generally, EBCs and WBCs are characterized by narrow shelves that are connected to much larger watersheds (Fig. 4b). Moreover, it can be observed that many EBCs and WBCs present relatively narrow watersheds too, in particular in the Pacific (CAL and HUM, Fig. 5a, b). The cumulative surface area of shelves under influence of boundary currents is 4.4×10^6 km^2 only (14 % of the world's total). The regional contributions vary widely from the very wide China Sea (CSK) on the one hand to the very narrow coastal ribbon following South America in the Southern Pacific on the other hand (HUM). In the Atlantic, the coasts of Morocco (MOR) and Portugal (IBE) are also very narrow, while those of the Eastern US (FLO), Brazil (BRA) and Namibia (SWA) extend over several tens of kilometers.

Margins under monsoonal influence are essentially located between the equator and the tropic of Cancer (23° N). A large section of this coastline is dominated by arid regions, on the Western side (WAS, Fig. 5d). The cumulative estuarine surface area in these regions is only 43×10^3 km^2, consisting mostly of small deltas located on the Indian sub-continent (EAS, Fig. 5d). The shelves are generally narrow while several watersheds are very large, in particular those flowing into the Bay of Bengal (BEN, Fig. 5e) like those of the Ganges-Brahmaputra, Godavari and Krishna rivers.

Sub-polar margins present a wide diversity of profiles with extended shallow shelves (North Sea, NEA, Patagonian shelf, SAM) as well as fragmented archipelagos (Labrador Sea). Their cumulative watershed area amounts to 9.5×10^6 km^2 and the ratio of watershed to shelf surface varies from 1 in New Zealand (NWZ) to 8 in the Labrador Sea (LAB) with an average value of 2.4. Estuaries in sub-polar regions essentially consist of tidal systems and fjords at the highest latitudes (NWP, NEP, Fig. 5a).

Polar margins are very wide as well as deep and account for over 50 % of the volume of the coastal ocean and 29 % of its surface area (Fig. 4). Although these systems include watersheds of several very large Russian rivers (Ob, Yenisei, Lena, Amur...), the average watershed to shelf ratio is only 2, the lowest amongst the classes of margins.

Most of the fjords of the world are located in Polar Regions and, while they represent 40 % of the world's estuarine surface area (Fig. 6), their cumulative contribution remains fairly small compared to the very wide arctic shelves. Locally, however, they may contribute significantly to the surface area, as in the case of Norway where some of the largest and deepest fjords are located and where the shelf breaks only a few kilometers offshore. Here, fjords account for a surface area as high as 10 % to that of the shelf.

Marginal seas, like sub-polar margins, do not exhibit a clear geomorphological pattern. $28 \times 10^6\ km^2$ of watershed are connected to marginal seas, which amounts to 21 % of the surface of the continents. Shallow internal seas (HUD, BAL, PER) have a very large surface area while most other marginal seas consist of narrow shelves collecting very large watersheds. This includes the Mississippi, the Nile and the Danube rivers, which discharge into the Gulf of Mexico (MEX), the Mediterranean Sea (MED) and the Black Sea (BLA), respectively. The Sea of Okhotsk (OKH) is an exception as it is characterized by a wide shelf ($10^6\ km^2$) connected to a relatively modest watershed of $2.4 \times 10^6\ km^2$.

Tropical margins are generally very narrow along the coasts of Africa (TEA and TWI) and America (TEP and TWA) and connected to some of the widest watersheds in the world (Amazon, Congo River, Niger). Their cumulative shelf surface area is $1.3 \times 10^6\ km^2$ for a cumulative watershed surface of $19.4 \times 10^6\ km^2$. Tropical margins in Oceania (TEI, NAU and SEA) display an opposite trend. The cumulative surface areas for shelves and watershed in this region are $4.9 \times 10^6\ km^2$ and $7.4 \times 10^6\ km^2$, respectively, yielding a ratio of 1.5. This is an order of magnitude lower than that of the other tropical margins and the average ratio is thus on the order of 4. Generally, the tropical MARCATS do not exhibit very large estuaries because their coastline is either dominated by small deltas or wide arheic regions (Dürr et al., 2011) where rivers do not flow constantly and occasional rain events create wadies rather than permanent estuaries. The latter is characteristic of regions such as, for example, the western coast of the Arabic Sea (WAS, Atroosh and Moustafa, 2012).

HESSD
9, 11319–11361, 2012

The cumulative surface area of MARCATS shelves integrated to the 350 m isobaths is shown in small panels on Fig. 5. The most common distribution displays a rapid increase in cumulative surface area up to isobaths 100–150 m. At this depth, 80 % of the total shelf area is accounted for and the increase is then more progressive. However, some MARCATS possess distinct features with a slope that increases linearly with depth. They belong mainly to the polar and sub-polar classes (NOR, LAB, NWZ) or to boundary currents (FLO, HUM, TEA). The peculiar profile of MARCATS 23 (TEA) is strongly influenced by the deep coastal canyon created by the Congo River (Droz et al., 1996). Other significant exceptions to the typical hypsometric profile include the Baltic Sea (BAL), the Black Sea (BLA) and the Persian Gulf (PER). All are shallow marginal seas which do not exhibit a real shelf break.

3.4 Water flows

The annually averaged freshwater discharges into the coastal ocean were calculated for each COSCAT and MARCATS (Table 3). The data set used is GlobalNEWS2 (Mayorga et al., 2010) from an original compilation of Fekete et al. (2002). Within each MARCATS, the discharge flowing through each estuarine type is also calculated (Fig. 5). The well-known hotspots for fresh water discharge are easily identified: the Amazon region (TWA), the Congo Region (TEA), the Bengal Bay fueled by the Ganges-Brahmaputra River (BEN) and South East Asia/Oceania (TEI, NAU and SEA). All these regions are located in the tropics and their segment is thus listed as tropical in Liu's classification except for BEN which is under monsoon influence. Polar and sub-polar regions do not provide as much fresh water, with the exception of MARCATS 44 (BKS) which collects the discharge of the Ob River. The Gulf of Mexico (MEX) is the only marginal sea that receives more than $1000 \times 10^3\,km^3\,yr^{-1}$ of fresh water, and to a large extent, this is due to the Mississippi River (Table 3). Together, the nine marginal systems contribute to 13 % of the world's river discharge.

In most segments fed by at least one large river, the fresh water input is largely dominated by its discharge (CAN, MEX, CAL, TWA, TEA, AGU, SIB, BEN, TEI). Similarly,

Discussion Paper | Discussion Paper | Discussion Paper | Discussion Paper |

HESSD

9, 11319–11361, 2012

Global multi-scale segmentation of continental and coastal waters

G. G. Laruelle et al.

regions where tidal estuaries are present tend to be dominated by these systems. This concerns, in particular, the Atlantic coast of the USA (LAB and FLO), the Brazilian current (BRA), Western Europe (NEA and IBE), The Barent and Kara Seas (BKS), the Okhotsk Sea (OKH), the Eastern China Sea (CSK) and Northern Australia (NAU). Fjords are exclusively found at high latitudes (NEP, SAM, CAN, HUD, LAB, NGR, SGR, NEA, NOR, BAL, BKS, NWZ) and, although their integrated surface area is important, their fresh water flow is quite modest (~ 7 % of the world total). Lagoons are found on most continents and all latitudes (Fig. 4) but, in terms of fresh water inputs, are only marginal contributors except in the Caribbeans (CAR) and along the Gulf of Mexico (MEX) where they can be found along stretches of the coastline and intercept ~ 40 % of the riverine water discharge. Small deltas, on the other hand, can locally be the main estuarine type through which significant water flow is transported. They are mainly located in tropical and sub-tropical areas and contribute very actively to highly rheic regions like the South East Asia and Oceania (SEA, TEI, NAU).

The residence time of fresh water in the continental shelf seas was calculated for each COSCAT and MARCATS by dividing each shelf volume by the corresponding riverine discharge (Fig. 5a–f). The global volume of continental shelf seas is $3860 \times 10^3\,km^3$, compared to the $39 \times 10^3\,km^3\,yr^{-1}$ of annual fresh water input into the ocean. This thus gives an average residence time of ~ 100 yr for fresh waters in continental shelf seas. However, this residence time is somewhat skewed by the very large contribution of Antarctic shelves to the total. If they are excluded from the calculation, the residence time drops to ~ 55 yr. This value is nonetheless higher than the average residence time of ~ 8–10 yr calculated on the basis of the exchange with the open ocean through upwelling fluxes (Brink et al., 1995; Rabouille et al., 2001; Ver, 1998). These estimates are based on globally averaged box-models and it should be remembered that the intensity of upwelling processes varies greatly in space and time and the water can locally be renewed in just weeks (Gruber et al., 2011). These calculations do not account either for lateral transport through coastal currents but the general scheme suggests that the renewal of continental shelf waters is 1 to 2 orders

HESSD
9, 11319–11361, 2012

of magnitude slower through riverine fresh water inputs than through upwelling fluxes. 17 of the 149 COSCATs have fresh water residence times shorter than 10 yr and 11 out of the 41 large rivers (Type V) flow into these segments. The cumulative annual fresh water input of these 17 COSCAT segment amounts to 16×10^3 km^3, which is 41 % of the global water flux. Because many of the largest rivers in the world reach the ocean at low latitudes, the fresh water residence time on tropical shelves is generally < 100 yr. Due to their narrow shelves, most of the African coast have low fresh water residence times (< 40 yr) as have most Pacific coasts.

4 Conclusions and outlook

In this study, a three level segmentation of the land-ocean continuum extending from the watersheds to the shelf break has been proposed. Levels II and III are used to construct large regional entities which retain the most important climatic, morphological and hydrological characteristics of continental waters and the coastal ocean. The resulting number of units (149 COSCATs and 45 MARCATS) can easily be manipulated and allows for comparison with existing segmentations for selected compartments of the land-ocean-continuum. The segments are well-constrained geographically and provide globally consistent estimates of hypsometric profiles, surface areas and volumes. A spatially resolved representation of the hydrological cycle from the river networks to the coastal ocean is also achievable as well as a qualitative treatment of the water flow routing through the different estuarine types.

The 0.5° resolution of our level I compares to the highest resolution globally available for global hydrological models and watershed GIS models. At this resolution, the vast majority of river networks are properly represented (Beusen et al., 2005). In addition, important global data bases cluster information the same resolution of 0.5–1° (World Ocean Atlas; Da Silva, 1994; Hexacoral), making combination and meta-analysis between data sets relatively easy. This is true for both the land and ocean compartments of the land-ocean-continuum (LOICZ, Crossland et al., 2005). Recent coastal analyses and typologies (Dürr et al., 2011) have also been performed using average properties calculated at similar resolution.

The multi-scale segmentation of the Land-Ocean-continuum provides an appropriate support for the progressive integration of global databases for carbon, nutrients and green house gas characteristics into lateral land-ocean matter flux budgets (Cai, 2011; Chen et al., 2012; Crossland et al., 2005; Gordon et al., 1996; Laruelle et al., 2010; Nixon et al., 1996) and, thus, to carry robust regional and global budgets of relevance to environmental and climatic research. In addition the dataset provided can be used to integrate the still missing recognition of lateral biogeochemical matter fluxes into Earth System Models of high resolution and better understand their influence on global biogeochemical cycles.

Supplementary material related to this article is available online at: http://www.hydrol-earth-syst-sci-discuss.net/9/11319/2012/ hessd-9-11319-2012-supplement.zip.

Acknowledgements. The research leading to these results has received funding from the European Union's Seventh Framework Program (FP7/2007–2013) under grant agreement no 283080, project GEOCARBON, by King Abdullah University of Science and Technology (KAUST) Center-in-Development Award to Utrecht University: project No. KUK-C1-017-12 and by the government of the Brussels-Capital Region (Brains Back to Brussels award to PR) and by the the German Science Foundation DFG (DFG-project HA 4472/6-1) and the Cluster of Excellence "CliSAP" (DFG, EXC177), Universität Hamburg. HHD received funding from NSERC (Canada Excellence Research Chair in Ecohydrology – Philippe van Cappellen).

HESSD

9, 11319–11361, 2012

References

Alongi, D. M.: Coastal Ecosystem Processes, CRC Press, New York, USA, 419 pp., 1998.

Anderson, J. B.: Antarctic Marine Geology, Cambridge University Press, Cambridge, p. 292, 1999.

Arndt, S., Vanderborght, J.-P., and Regnier, P.: Diatom growth response to physical forcing in a macrotidal estuary: coupling hydrodynamics, sediment transport, and biogeochemistry, J. Geophys. Res., 112, 1–23, doi:10.1029/2006JC003581, 2007.

Arndt, S., Regnier, P., and Vanderborght, J.-P.: Seasonally-resolved nutrient export fluxes and filtering capacities in a macrotidal estuary, J. Marine Syst., 78, 42–58, doi:10.1016/j.jmarsys.2009.02.008, 2009.

Arndt, S., Lacroix, G., Gypens, N., Regnier, P., and Lancelot, C.: Nutrient dynamics and phytoplankton development along an estuary–coastal zone continuum: a model study, J. Marine Syst., 84, 49–66, doi:10.1016/j.jmarsys.2010.08.005, 2011.

Atkinson, L. P., Huthnance, J. M., and Blanco, J. L.: Circulation, mixing and the distribution of remineralized nutrients, in: The Sea, vol. 13, edited by: Robinson, A. R. and Brink, K. H., Harvard University Press, Cambridge, Mass., 227–268, 2005.

Atroosh, K. B. and Moustafa, A. T.: An estimation of the probability distribution of Wadi Bana flow in the Abyan Delta of Yemen, J. Agr. Sci., 4, 80–89, doi:10.5539/jas.v4n6p80, 2012.

Beusen, A. H. W., Dekkers, A. L. M., Bouwman, A. F., Ludwig, W., and Harrison, J.: Estimation of global river transport of sediments and associated particulate C, N, and P, Global Biogeochem. Cy., 19, doi:10.1029/2005GB002453, 2005.

Brink, K. H., Abrantes, F. F. G., Bernal, P. A., Dugdale, R. C., Estrada, M., Hutchings, L., Jahnke, R. A., Muller, P. J., and Smith, R. L.: Group report: how do coastal upwelling systems operate as integrated physical, chemical, and biological systems and influence the geological record?, in: Upwelling in the Ocean: Modern Processes and Ancient Records, edited by: Summerhayes, C. P., Emeis, K.-C., Angel, M. V., Smith, R. L., and Zeitzeschel, B., John Wiley & Sons, New York, 103–124, 1995.

Borges, A. V., Delille, B., and Frankignoulle, M.: Budgeting sinks and sources of CO_2 in the coastal ocean: diversity of ecosystems counts, Geophys. Res. Lett., 32, L14601, doi:10.1029/2005GL023053, 2005.

Cai, W. J.: Estuarine and coastal ocean carbon paradox: CO_2 sinks or sites of terrestrial carbon incineration?, Annu. Rev. Marine Sci., 3, 123–145, 2011.

Cai, W. J., Dai, M. H., and Wang, Y. C.: Air sea exchange of carbon dioxide in ocean margins: a province based synthesis, Geophys. Res. Lett., 33, L12603, doi:10.1029/2006GL026219, 2006.

CIA: The World Factbook, available at: https://www.cia.gov/library/publications/the-world-factbook/fields/2060.html (last access: 27 September 2012), 2009.

Crossland, C. J., Kremer, H. H., Lindeboom, H. J., Marshall Crossland, J. I., and LeTissier, M. D. A.: Coastal Fluxes in the Anthropocene, Global Change – The IGBP Series, Springer, Berlin, Heidelberg, 2005.

Droz, L., Rigaut, F., Cochonat, P., and Tofani, R.: Morphology and recent evolution of the Zaire turbidite system (Gulf of Guinea), Bull. Geol. Soc. Am., 108, 253–269, 1996.

Dürr, H. H., Laruelle, G. G., van Kempen, C. M., Slomp, C. P., Meybeck, M., and Middelkoop, H.: Worldwide typology of nearshore coastal systems: defining the estuarine filter of river inputs to the oceans, Estuar. Coasts, 34, 441–458, doi:10.1007/s12237-011-9381-y, 2011.

Elliott, M. and McLusky, D. S.: The need for definitions in understanding estuaries, Estuar. Coast. Shelf S., 55, 815–827, 2002.

Fekete, B. M., Vörösmarty, C. J., and Grabs W.: High-resolution fields of global runoff combining observed river discharge and simulated water balances, Global Biogeochem. Cy., 16, 1042, doi:10.1029/1999GB001254, 2002.

Gordon, J. D. C., Boudreau, P. R., Mann, K. H., Ong, J. E., Silvert, W. L., Smith, S. V., Wattayakorn, G., Wulff, F., and Yanagi, T.: LOICZ biogeochemical modelling guidelines, LOICZ reports & studies, 5, LOICZ, Texel, 1996.

Gattuso, J.-P., Frankignoulle, M., and Wollast, R.: Carbon and carbonate metabolism in coastal aquatic ecosystems, Annu. Rev. Ecol. Syst., 29, 405–433, 1998.

Gross, G. M.: Oceanography: A View of the Earth, Prentice-Hall, Inc., Englewood Cliffs, 1972.

Gruber, N., Lachkar, Z., Frenzel, H., Marchesiello, P., Munnich, M., McWilliams, J. C., Nagai, T., and Plattner, G.-K.: Mesoscale eddy-induced reduction in eastern boundary upwelling systems, Nat. Geosci., 4, 787–792, 2011.

Jahnke, R. A.: The global ocean flux of particulate organic carbon: areal distribution and magnitude, Global Biogeochem. Cy., 10, 71–88, 1996.

Jacobs, S. S., Helmer, H. H., Doake, C. S. M., Jenkins, A., and Frolich, R. M.: Melting of ice shelves and the mass balance of Antarctica, J. Glaciol., 38, 375–387, 1992.

Karl, D. M.: A sea of change: biogeochemical variability in the North Pacific Subtropical Gyre, Ecosystems, 2, 181–214, 1999.

Lambeck, K. and Chappell, J.: Sea level change through the last glacial cycle, Science, 292, 679–686, 2001.
Laruelle, G. G.: Quantifying nutrient cycling and retention in coastal waters at the global scale, PhD dissertation, Utrecht University, Utrecht, The Netherlands, 2009.
Laruelle, G. G., Roubeix, V., Sferratore, A., Brodherr, B., Ciuffa, D., Conley, D. J., Dürr, H. H., Garnier, J., Lancelot, C., Le Thi Phuong, Q., Meunier, J.-D., Meybeck, M., Michalopoulos, P., Moriceau, B., Ní Longphuirt, S., Loucaides, S., Papush, L., Presti, M., Ragueneau, O., Regnier, P. A. G., Saccone, L., Slomp, C. P., Spiteri, C., and Van Cappellen, P.: The global biogeochemical cycle of silicon: role of the land-ocean transition and response to anthropogenic perturbation, Global Biogeochem. Cy., 23, GB4031, doi:10.1029/2008GB003267, 2009.
Laruelle, G. G., Durr, H. H., Slomp, C. P., and Borges, A. V.: Evaluation of sinks and sources of CO_2 in the global coastal ocean using a spatially-explicit typology of estuaries and continental shelves, Geophys. Res. Lett., 37, L15607, doi:10.1029/2010GL043691, 2010.
Liu, K.-K., Atkinson, L., Quiñones, R., and Talaue-McManus, L. (Eds.): Carbon and Nutrient Fluxes in Continental Margins, Global Change – The IGBP Series, 3, Springer-Verlag, Berlin, Heidelberg, doi:10.1029/2002WR001619, 2010.
Longhurst, A.: Seasonal cycles of pelagic production and consumption, Prog. Oceanogr., 36, 77–167, 1995.
Longhurst, A.: Ecological geography of the sea, Academic Press, San Diego, 398 pp., 1998.
Mackenzie, F. T.: Global carbon cycle: Some minor sinks for CO_2, in: Flux of Organic Carbon from the Major Rivers of the World to the Oceans, edited by: Likens, G. E., Mackenzie, F. T., Richey, J. E., Sedwell, J. R., and Turekian, K. K., NAS Report, Washington, DC, 360–384, 1981.
Mackenzie, F. T., Ver, L. M., and Lerman, A.: Century-scale nitrogen and phosphorus controls of the carbon cycle, Chem. Geol., 190, 13–32. 2002.
Mackenzie, F. T., Andersson, A., Lerman, A., and Ver, L. M.: Boundary exchanges in the global coastal margin: implications for the organic and inorganic carbon cycles, in: The Sea, 13, Chap. 7, edited by: Robinson, A. R. and Brink, K. H., Harvard University Press, Cambridge, MA, 193–225, 2005.
Mann, K. H. and Lazier, J. R. N.: Dynamics of Marine Ecosystems: Biological-Physical Interactions in the Oceans, 3rd Edn., Blackwell Publishing, New York, 2006.

Mayorga, E., Seitzinger, S. P., Harrison, J. A., Dumont, E., Beusen, A. H. W., Bouwman, A. F., Fekete, B. M., Kroeze, C., and Van Drecht, G.: Global nutrient export from watersheds 2 (NEWS 2): model development and implementation, Environ. Modell. Softw., 25, 837–853, doi:10.1016/j.envsoft.2010.01.007, 2010.

McKee, B. A., Aller, R. C., Allison, M. A., Bianchi, T. S., and Kineke, G. C.: Transport and transformation of dissolved and particulate materials on continental margins influenced by major rivers: benthic boundary layer and seabed processes, Cont. Shelf Res., 24, 899–926, 2004.

Meybeck, M. and Dürr, H. H.: Cascading filters of river material from headwaters to regional seas: the european example, in: Watersheds, Bays, and Bounded Seas – The Science and Management of Semi-Enclosed Marine Systems, SCOPE Series 70, edited by: Urban Jr., E. R., Sundby, B., Malanotte-Rizzoli, P., and Melillo, J. M., 115–139, Island Press, Washington, 2009.

Meybeck, M., Dürr, H. H., and Vörosmarty, C. J.: Global coastal segmentation and its river catchment contributors: a new look at land-ocean linkage, Global Biogeochem. Cy., 20, GB1S90, 1–15, doi:10.1029/2005GB002540, 2006.

Meybeck, M., Dürr, H. H., Roussennac, S., and Ludwig, W.: Regional seas and their interception of riverine fluxes to oceans, Mar. Chem., 106, 301–325, 2007.

Nag, P.: Coastal geomorphic features around Indian Ocean, Indian J. Geo-Mar. Sci., 39, 557–561, 2010.

New York Times: Times atlas of the world: Comprehensive edition, 9th Edn., New York Times, New York, 1992.

Nixon, S. W., Ammenman, J. W., Atkinson, L. P., Berounsky, V. M., Billen, G., Boicourt, W. C., Boynton, W. R., Church, T. M., DiToro, D. M., Elmgren, R., Garber, J. H., Giblin, A. E., Jahnke, R. A., Owens, N. J. P., Pilson, M. E. J., and Seitzinger, S. P.: The fate of nitrogen and phosphorus at the land sea margin of the North Atlantic Ocean, Biogeochemistry, 35, 141–180, 1996.

Pinet, P. R.: Invitation to Oceanography, 3rd Edn., West Publishing Co., St. Paul, MN, 1996.

Rabouille, C., Mackenzie, F. T., and Ver, L. M.: Influence of the human perturbation on carbon, nitrogen, and oxygen biogeochemical cycles in the global coastal ocean, Geochim. Cosmochim. Ac., 65, 3615–3641, 2001.

Pearce, A. F.: The Leeuwin Current and the Houtman Abrolhos Islands, Western Australia, in: The Marine Flora and Fauna of the Houtman Abrolhos Islands, Western Australia, vol. 1, edited by: Wells, F. E., Western Australian Museum, Perth, 11–46, 1997.

Regnier, P. and Steefel, C. I.: A high resolution estimate of the inorganic nitrogen flux from the Scheldt estuary to the coastal North Sea during a nitrogen-limited algal bloom, spring 1995, Geochim. Cosmochim. Ac., 63, 1359–1374, 1999.

Schwartz, M. L.: Encyclopedia of coastal science, Springer, Dordrecht, 2005.

Seiter, K., Hensen, C., and Zabel, M.: Benthic carbon mineralization on a global scale, Global Biogeochem. Cy., 19, GB1010, doi:10.1029/2004GB002225, 2005.

Seitzinger, S. P., Harrison, J. A., Dumont, E., Beusen, A. H. W., and Bouwman, F. B. A.: Sources and delivery of carbon, nitrogen, and phosphorus to the coastal zone: an overview of global nutrient export from watersheds (NEWS) models and their application, Global Biogeochem. Cy., 19, GB4S01, doi:10.1029/2005GB002606, 2005.

Sherman, K. and Alexander, L. M. (Eds.): Biomass yields and geography of large marine ecosystems, Am. Assoc. Adv. Sci. Sel. Symp. 111, Boulder, CO, Westview Press, p. 449, 1989.

Sherman, K.: The large marine ecosystem concept: research and management strategy for living marine resources, Ecol. Appl., 1, 350–360, 1991.

Slomp, C. P. and Van Cappellen, P.: Nutrient inputs to the coastal ocean through submarine groundwater discharge: controls and potential impact, J. Hydrol., 295, 64–86, 2004.

Smith, S. V. and Hollibaugh, J. T.: Coastal metabolism and the oceanic carbon balance, Rev. Geophys., 31, 75–89. 1993.

Smith, W. H. F. and Sandwell, D. T.: Global Seafloor Topography from Satellite Altimetry and Ship Depth Soundings, version 9.1b, available at: http://topex.ucsd.edu/marine_topo/ (last access: 20 December 2007), 1997.

Tsandev, I., Rabouille, C., Slomp, C. P., and Van Cappellen, P.: Shelf erosion and submarine river canyons: implications for deep-sea oxygenation and ocean productivity during glaciation, Biogeosciences, 7, 1973–1982, doi:10.5194/bg-7-1973-2010, 2010.

US Department of Commerce, National Oceanic and Atmospheric Administration, National Geophysical Data Center: 2-minute Gridded Global Relief Data (ETOPO2v2), 2006, available at: http://www.ngdc.noaa.gov/mgg/fliers/06mgg01.html, last accessed: 26 December 2008.

HESSD
9, 11319–11361, 2012

Vanderborght, J. P., Wollast, R., Loijens, M., and Regnier, P.: Application of a transport-reaction model to the estimation of biogas fluxes in the Scheldt estuary, Biogeochemistry, 59, 207–237, 2002.

Vanderborght, J. P., Folmer, I., Aguilera, D. R., Uhrenholdt, T., and Regnier, P.: Reactive-transport modelling of a river-estuarine-coastal zone system: application to the Scheldt estuary, Mar. Chem., 106, 92–110, 2007.

Ver, L. M.: Global kinetic models of the coupled C, N, P, and S biogeochemical cycles: implications for global environmental change, Ph.D. dissertation, University of Hawaii, Hawai, 1998.

Vörösmarty, C. J., Fekete, B. M., Meybeck, M., and Lammers, R. B.: The global system of rivers: its role in organizing continental land mass and defining land-to-ocean linkages, Global Biogeochem. Cy., 14, 599–621, 2000a.

Vörösmarty, C. J., Fekete, B. M., Meybeck, M., and Lammers, R. B.: Geomorphometric attributes of the global system of rivers at 30-minute spatial resolution, J. Hydrol., 237, 17–39, 2000b.

Walsh, J. J.: On the Nature of Continental Shelves, Academic Press, San Diego, New York, Berkeley, Boston, London, Sydney, Tokyo, Toronto, 1988.

Wollast, R.: Evaluation and comparison of the global carbon cycle in the coastal zone and in the open ocean, in: The Global Coastal Ocean, edited by: Brink, K. H. and Robinson, A. R., John Wiley & Sons, New York, 213–252, 1998.

Woodwell, G. M., Rich, P. H., and Hall, C. A. S.: Carbon in estuaries, in: Carbon and the biosphere, edited by: Woodwell, G. M. and Pecan, E. V., Technical Information Center, Office of Information Services, United States Atomic Energy Commission, Springfield, Virginia, 221–240, 1973.

Xie, L. and Hsieh, W. W.: Global wind-induced upwelling, Fish. Oceanogr., 4, 52–67, 1975.

HESSD

9, 11319–11361, 2012

Global multi-scale segmentation of continental and coastal waters

G. G. Laruelle et al.

Table 1. Global surface areas and volumes of coastal seas between various isobaths. The integrated values between the shore and the deepest isobaths are also provided.

Depth (m)	Surface (10^6 km^2)	Cumulative	Volume (10^6 km^3)	Cumulative
0–20	4.969		0.053	
20–50	7.413	12.379	0.260	0.312
50–80	5.100	17.480	0.330	0.643
80–120	4.306	21.786	0.428	1.070
120–150	2.124	23.909	0.287	1.358
150–200	2.476	26.386	0.434	1.792
200–350	4.550	30.937	1.234	3.026
350–500	3.083	34.020	1.307	4.333
500–750	3.401	37.421	2.098	6.432
750–1000	2.417	39.838	2.113	8.545
Total	39.838		8.545	

HESSD
9, 11319–11361, 2012

Table 2. List of the modified COSCAT segments with the depth of the outer limit of their continental shelves and the residence time of fresh water. COSCATs followed by a star (*) have been defined or modified for the purpose of the present work.

MARCATS	COSCAT	Shelf limit (m)	Fresh Water Residence time (yr)	MARCATS	COSCAT	Shelf limit (m)	Fresh Water Residence time (yr)
1-NEP	0809	350	29.6	9-MEX	0832	150	40.6
	0810	350	87.2		0833	200	74.0
	0811	500	1552.1		0834	120	11.6
2-CAL	0804	150	42.2	10-FLO	0826	150	261.2
	0805	200	428.1		0827	150	75.2
	0806	200	4340.1		0828	120	41.9
	0807	200	33.7	11-LAB	0821	500	164.4
	0808	350	12.5		0822	120	57.3
3-TEP	0801	150	34.6		0824	120	14.7
	0802	350	89.3		0825	150	12.9
	0803	80	4.9	12-HUD	0817	–	226.9
	1115	150	33.6		0818	–	8.6
	1116	150	5.7		0819	–	375.8
4-HUM	1112*	350	43.5		0820	–	531.6
	1113	200	239.8	13-CAN	0814	150	2055.4
	1114	500	1044.3		0815	120	24.6
5-SAM	1109	350	367.5		0816	500	2596.8
	1110	350	3502.1		0823	80	–
	1111*	500	142.8	14-NGR	0501	500	2808.0
6-BRA	1106	120	18.5		0502	500	1960.0
	1107	350	130.2		0505	500	1367.9
	1108	350	9.8	15-SGR	0503	500	1369.9
7-TWA	1103	150	2.8		0504	500	166.7
	1104	200	1.8	16-NOR	0407	200	92.4
	1105	120	21.3	17-NEA	0402	350	371.8
8-CAR	0830	120	9.3		0403	200	113.0
	0831	120	12.1	18-BAL	0404	–	110.1
	1101	150	3.4		0405	–	40.1
	1102	350	155.1		0406	–	9.1

HESSD
9, 11319–11361, 2012

Table 2. Continued.

MARCATS	COSCAT	Shelf limit (m)	Fresh Water Residence time (yr)	MARCATS	COSCAT	Shelf limit (m)	Fresh Water Residence time (yr)
19-IBE	0401	350	172.4	27-WIB	0005	120	1409.9
	0419*	350	62.1		0006	150	97.4
20-MED	0001	200	234.4		1341	150	3678.4
	0002	150	3525.9	28-RED	0004	150	762.0
	0003	150	8.3		1344	150	41071.0
	0414*	150	162.0	29-PER	1342	–	135.6
	0415	200	232.8	30-EIB	1338	150	48.8
	0416	350	76.7		1339	200	64.3
	0417	200	389.2		1340	200	86.1
	0418	200	69.6	31-BEN	1336	350	6.8
	1301*	150	40.3		1337	150	13.4
21-BLA	0411	–	13.0	32-TEI	1334	150	29.7
	0412	350	19.4		1335	200	18.6
	0413	350	593.0		1414	200	620.8
	1103	150	2.8	33-LEE	1413	350	848.5
22-MOR	0019	150	24.5	34-SAU	1411	350	261.1
	0020	150	11722.1		1412	350	2163.1
	0021	200	743.5	35-EAC	1410	350	181.8
23-TEA	0014	150	162.0	36-NWZ	1406	200	87.8
	0015	200	232.8		1407	350	282.7
	0016	350	76.7		1408	350	43.7
	0017	200	389.2		1409	350	81.1
	0018	200	69.6	37-NAU	1330	150	35.2
24-SWA	0013	750	5613.6		1333	200	52.5
25-AGU	0009	150	10.9		1401	200	7.7
	0010	120	15.8		1402	150	14.1
	0011	120	4.8		1403	500	88.7
	0012	350	421.0		1415	350	252.4
26-TWI	0007	120	3.1		1416	150	31.7
	0008	150	11.2	38-SEA	1328	200	40.2

HESSD
9, 11319–11361, 2012

Global multi-scale segmentation of continental and coastal waters

G. G. Laruelle et al.

Table 2. Continued.

MARCATS	COSCAT	Shelf limit (m)	Fresh Water Residence time (yr)	MARCATS	COSCAT	Shelf limit (m)	Fresh Water Residence time (yr)
38-SEA (Cont.)	1329	200	46.9	43-SIB	1309	150	13.7
	1331	150	23.1		1310*	150	261.0
	1332	350	98.6		1311*	500	352.4
39-CSK	1322	500	192.5		1312*	150	1563.2
	1323	150	24.4		1313	500	1697.0
	1324	–	517.5	44-BKS	0408	200	196.9
	1325	–	42.8		0409	200	3477.7
	1326	350	35.4		1307	500	97.6
40-JAP	1320	350	89.8		1308	500	61.0
	1321	500	223.8	45-ANT	1501*	1000	–
41-OKH	1317	750	1360.0		1502*	750	–
	1318	500	84.7		1503*	1000	–
	1319	500	569.5		1504*	1000	–
42-NWP	0812	350	321.8		1505*	1000	–
	1314	350	518.3				
	1315	350	195.5				
	1316	500	108.0				

HESSD
9, 11319–11361, 2012

Table 3. List of the MARCATS segments with their type, the surface area of their various components, the fresh water discharge and the volume of their continental shelves.

Number	System Name	Symbol	Class	Estuarine Surface ($10^3\,km^2$)	Watershed Surface ($10^3\,km^2$)	Shelf Surface ($10^3\,km^2$)	Fresh Water Discharge ($km^3\,yr^{-1}$)	Shelf Volume (km^3)
1	North Eastern Pacific	NEP	Subpolar	33.9	919	461	785	58 932
2	Californian Current	CAL	EBC	8.9	1781	214	428	16 668
3	Tropical Eastern Pacific	TEP	Tropical	6.2	638	198	586	15 777
4	Peruvian Upwelling Current	HUM	EBC	4.2	725	143	120	19 769
5	Southern America	SAM	Subpolar	22.0	1917	1230	289	141 652
6	Brazilian Current	BRA	WBC	26.3	4624	521	1117	36 214
7	Tropical Western Atlantic	TWA	Tropical	13.4	9242	517	8981	20 691
8	Caribbean Sea	CAR	Tropical	26.2	1109	344	941	15 721
9	Gulf of Mexico	MEX	Marginal Sea	31.9	5411	544	1085	22 432
10	Florida Upwelling	FLO	WBC	34.0	1130	858	531	50 522
11	Sea of Labrador	LAB	Subpolar	36.1	2351	395	1080	43 178
12	Hudson Bay	HUD	Margial Sea	39.0	3601	1064	666	105 267
13	Canadian Archipelagos	CAN	Polar	163.7	3725	1177	382	157 543
14	Northern Groenland	NGR	Polar	24.1	373	614	82	139 337
15	Southern Groenland	SGR	Polar	8.8	101	270	108	60 538
16	Norwegian Basin	NOR	Polar	17.0	219	171	183	16 915
17	North Eastern Atlantic	NEA	Marginal Sea	37.6	1089	1112	498	101 984
18	Baltic Sea	BAL	Marginal Sea	26.3	1619	383	376	20 165
19	Iberian Upwelling	IBE	EBC	12.7	818	283	202	26 640
20	Mediterranean Sea	MED	Marginal Sea	15.1	8168	580	674	42 224
21	Black Sea	BLA	Marginal Sea	10.3	2411	172	360	8246
22	Moroccan Upwelling	MOR	EBC	5.6	3637	225	125	11 520
23	Tropical Eastern Atlantic	TEA	Tropical	26.6	8394	284	2762	14 786
24	Southern Western Africa	SWA	EBC	1.7	1293	308	14	76 289
25	Agulhas Current	AGU	WBC	28.4	3038	254	657	19 607
26	Tropical Western Indian	TWI	Tropical	5.8	1022	72	328	2039
27	Western Arabian Sea	WAS	Indian Margins	2.0	1723	102	26	5234
28	Rea Sea	RED	Marginal Sea	0	771	190	6	8101
29	Persian Gulf	PER	Marginal Sea	2.3	2466	233	61	8296
30	Eastern Arabian Sea	EAS	Indian Margins	14.5	1847	342	293	18 823

HESSD
9, 11319–11361, 2012

Table 3. Continued.

Number	System Name	Symbol	Class	Estuarine Surface (10^3 km^2)	Watershed Surface (10^3 km^2)	Shelf Surface (10^3 km^2)	Fresh Water Discharge (km^3 yr^{-1})	Shelf Volume (km^3)
31	Bay of Bengal	BEN	Indian Margins	10.1	2934	230	1640	12 888
32	Tropical Eastern Indian	TEI	Indian Margins	16.2	2060	809	1324	48 634
33	Leeuwin Current	LEE	EBC	0.6	471	118	11	9707
34	Southern Australia	SAU	Subpolar	13.1	2249	452	66	38 307
35	Eastern Australian Current	EAC	WBC	7.9	290	139	67	12 149
36	New Zealand	NWZ	Subpolar	7.3	265	283	340	36 833
37	Northern Australia	NAU	Tropical	40.5	3010	2463	2548	145 236
38	South East Asia	SEA	Tropical	45.6	3343	2318	2872	155 848
39	China Sea and Kuroshio	CSK	WBC	27.8	4401	1299	1594	125 364
40	Sea of Japan	JAP	Marginal Sea	6.7	418	277	252	40 760
41	Sea of Okhotsk	OKH	Marginal Sea	19.7	2472	992	539	199 588
42	North Western Pacific	NWP	Subpolar	22.3	1783	1082	363	82 323
43	Siberian Shelves	SIB	Polar	37.8	5041	1918	801	123 368
44	Barent and Kara Seas	BKS	Polar	72.2	7940	1727	1585	181 707
45	Antarctic Shelves	ANT	Polar	–	–	2952	–	1 362 298

HESSD
9, 11319–11361, 2012

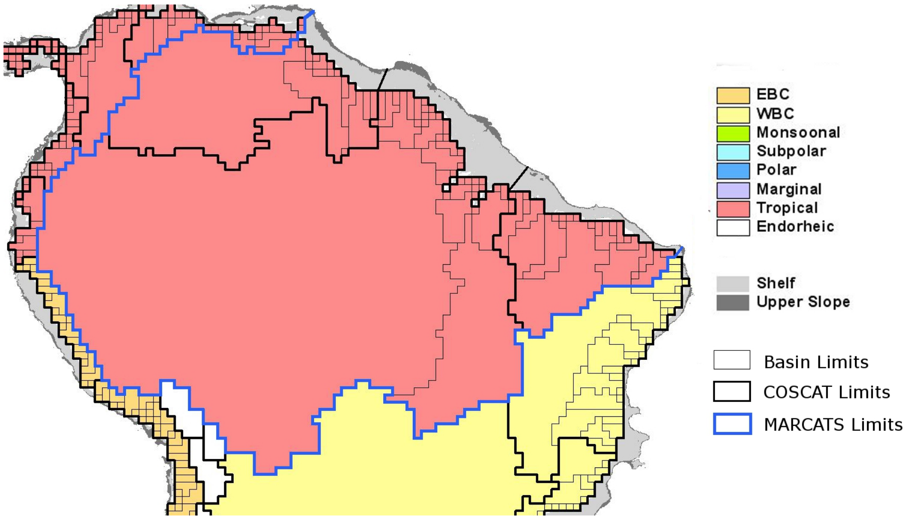

Fig. 1. Map of equatorial South America displaying the 3 layers of the segmentation and their boundaries (1- watersheds, 2- COSCATs, 3- MARCATS).

HESSD
9, 11319–11361, 2012

Global multi-scale segmentation of continental and coastal waters

G. G. Laruelle et al.

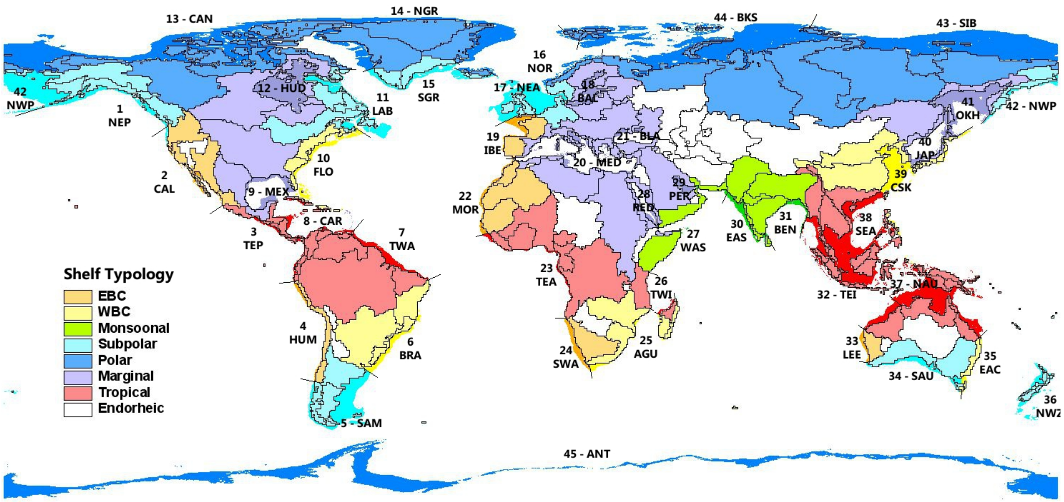

Fig. 2. Geographic limits of MARCATS and COSCAT segments with the typology or MARCATS.

HESSD
9, 11319–11361, 2012

Global multi-scale segmentation of continental and coastal waters

G. G. Laruelle et al.

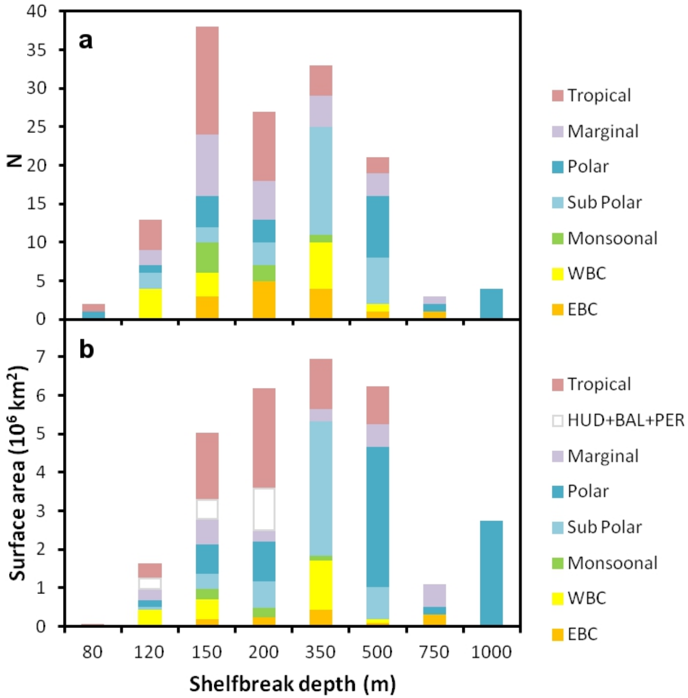

Fig. 3. Repartition of the depth at which the shelf breaks for each COSCAT segment **(a)** and integrated surface area continental shelves **(b)**. The colour code represents the type of MARCATS and the continental margins are highlighted by darker shades.

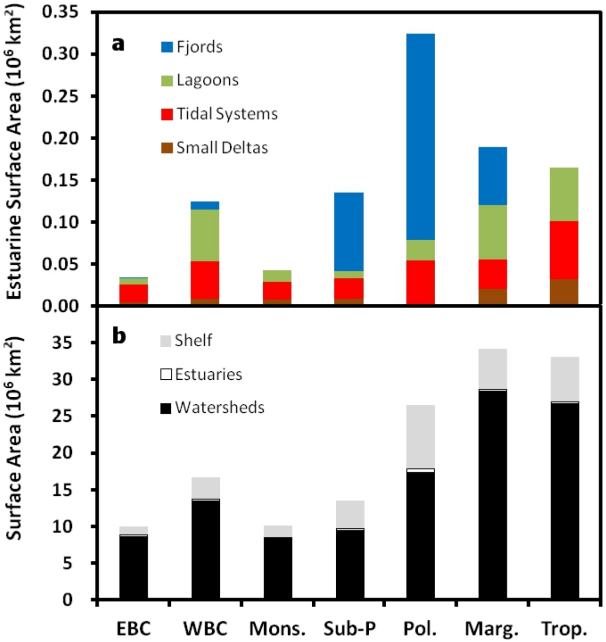

Fig. 4. Integrated surface areas for each MARCATS class of the different estuarine types **(a)** and watersheds, estuaries and continental shelf **(b)**.

HESSD
9, 11319–11361, 2012

Global multi-scale segmentation of continental and coastal waters

G. G. Laruelle et al.

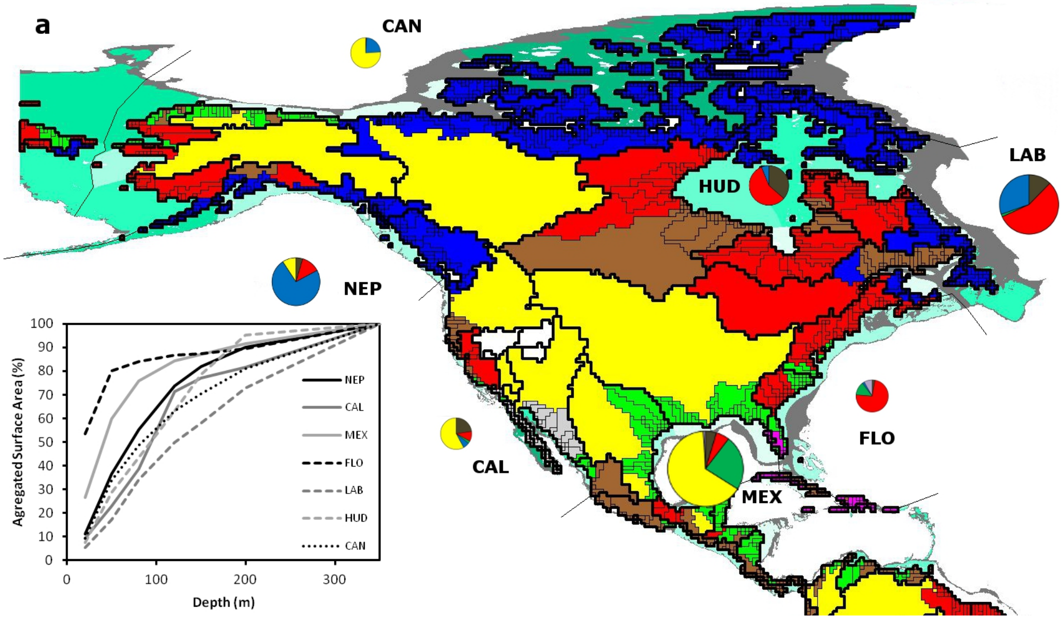

Fig. 5. Caption on p. 11360.

HESSD
9, 11319–11361, 2012

Global multi-scale segmentation of continental and coastal waters

G. G. Laruelle et al.

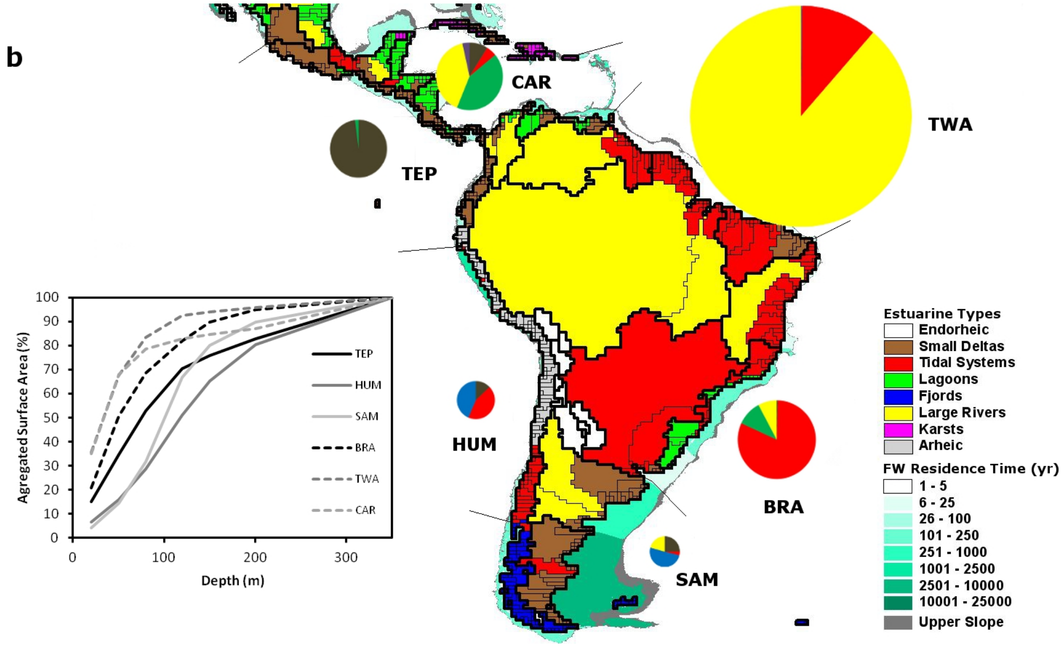

Fig. 5. Caption on p. 11360.

HESSD
9, 11319–11361, 2012

Global multi-scale segmentation of continental and coastal waters

G. G. Laruelle et al.

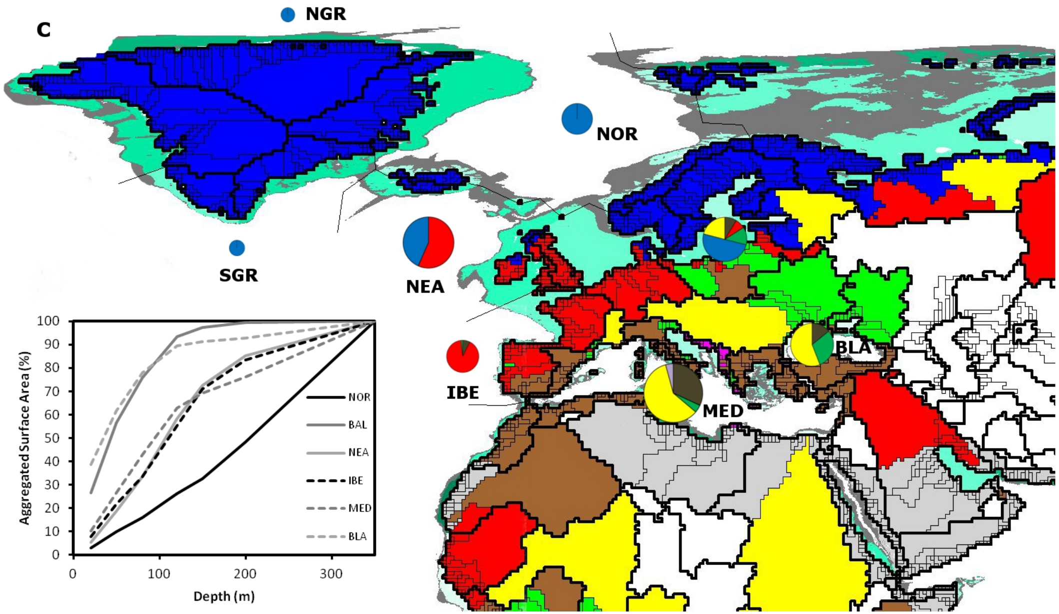

Fig. 5. Caption on p. 11360.

HESSD
9, 11319–11361, 2012

Global multi-scale segmentation of continental and coastal waters

G. G. Laruelle et al.

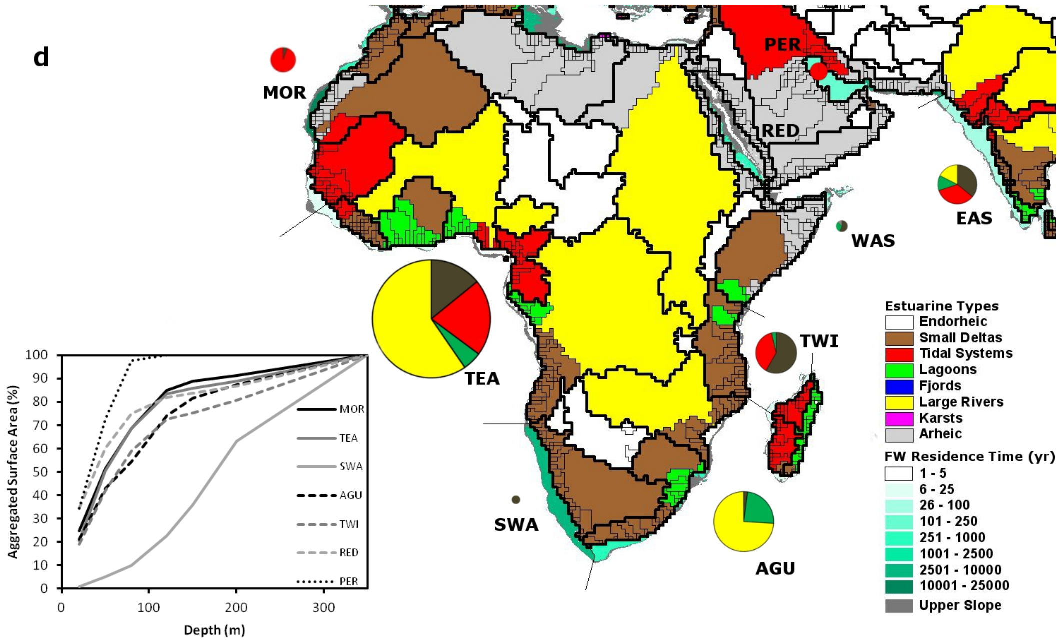

Fig. 5. Caption on p. 11360.

HESSD
9, 11319–11361, 2012

Global multi-scale segmentation of continental and coastal waters

G. G. Laruelle et al.

Title Page
Abstract Introduction
Conclusions References
Tables Figures
◀ ▶
Back Close
Full Screen / Esc
Printer-friendly Version
Interactive Discussion

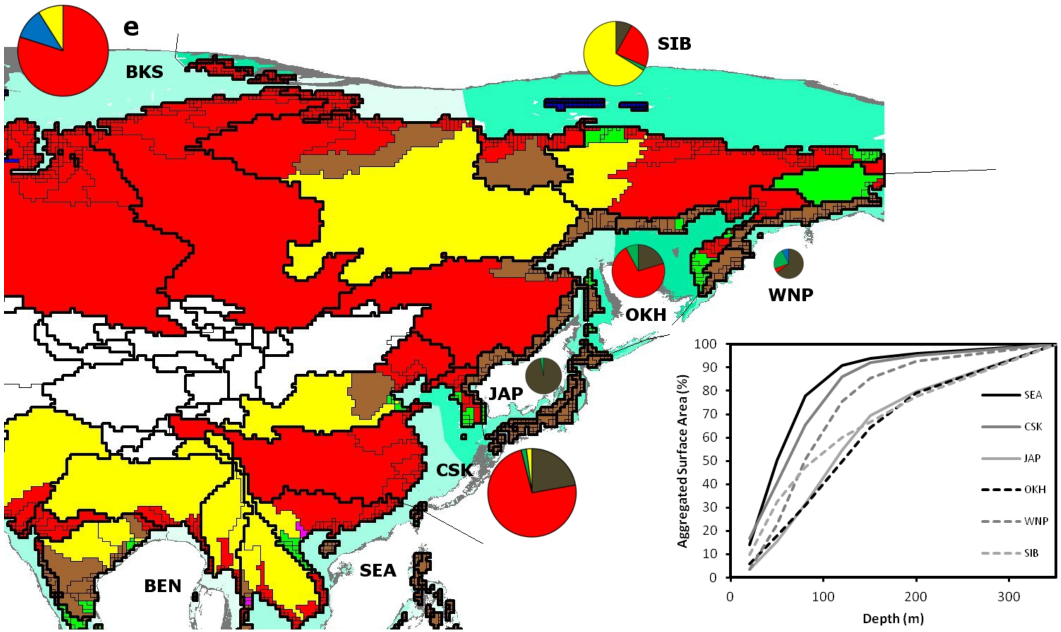

Fig. 5. Caption on p. 11360.

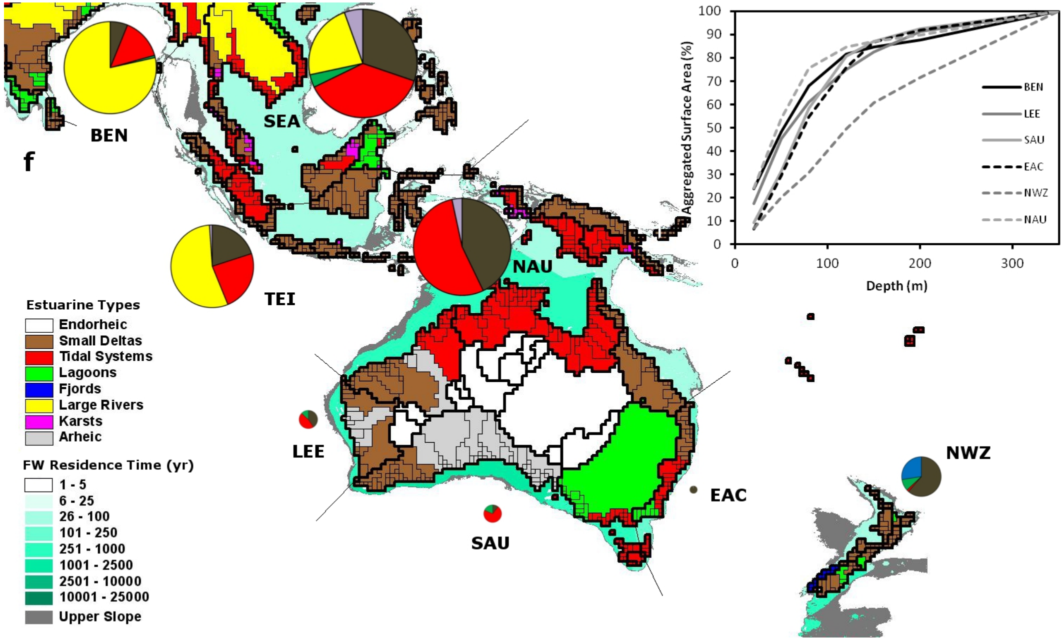

Fig. 5. Map representing the COSCAT segments (bold lines) and their corresponding continental shelf. The colour of the shelf indicates the fresh water residence time and the grey area represents the geographic extent of the upper slope (from the shelf break until the −1000 m isobaths). Within each COSCAT the limits of all watersheds are indicated at a 0.5° resolution and the colour code indicate the type of estuarine filter at the interface between the river and the shelf. The limits of the MARCATS segments are indicated by the grey lines and, for each one, a pie chart represents the total fresh water discharge from rivers and its distribution amongst the different estuarine types. The size of the pie is proportional to the total water discharge for a given MARCATS. The panel provides the integrated surface area of the shelf with respect to the depth of its outer limit for each MARCATS segment.

HESSD
9, 11319–11361, 2012

Global multi-scale segmentation of continental and coastal waters

G. G. Laruelle et al.

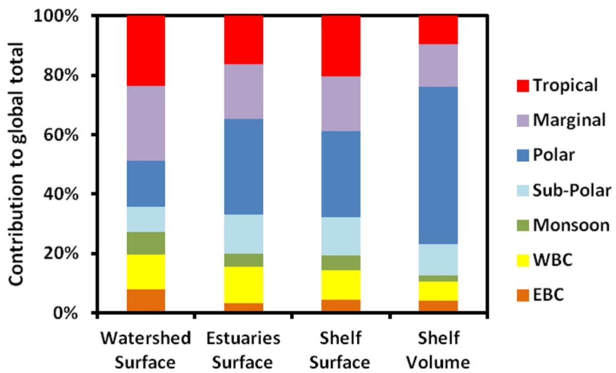

Fig. 6. Contribution of each MARCATS class to the global watershed surface area, estuarine surface area, continental shelf surface area and continental shelf volume.

HESSD
9, 11319–11361, 2012

Global multi-scale segmentation of continental and coastal waters

G. G. Laruelle et al.